The International Workshop on Mechatronics 2006
December 12-13, 2006, Supalai Resort, Saraburi, Thailand

Efficiency Improvement and Loss Analysis of Ultra-High Speed Permanent-Magnet Motor

Masaru Kano, and Toshihiko Noguchi

Department of Electrical Engineering, Faculty of Engineering,
Nagaoka University of Technology, 1603-1 Kamitomioka, Nagaoka, Niigata 940-2188, Japan
Tel/Fax: 81-258-47-9510, E-mail: kano@stn.nagaokaut.ac.jp, tnoguchi@vos.nagaokaut.ac.jp

Abstract

This paper describes a design of an ultra-high speed (UHS) permanent-magnet (PM) synchronous motor for a supercharger mounted on an automotive engine. Conventional superchargers are mechanically powered by the engine to compress inlet air to the engine cylinder. The supercharger electrically driven by the UHS motor allows employing a centrifugal compressor. It has higher efficiency and higher output pressure than a displacement compressor [1, 2]. Therefore, the electric supercharger can improve the efficiency of total drive system and output pressure response without mechanical linkage to the engine. In this paper, a surface permanent-magnet (SPM) motor (150,000 r/min, 1.5 kW) fed by a low voltage battery (12 V) is discussed. The simulation results through Finite Element Method (FEM) analysis are presented for an optimal permeance coefficient design and efficiency improvement.

Keywords: ultra-high speed PM motor, permeance coefficient, FEM analysis

1. Introduction

Automotive superchargers are mechanically linked to an internal combustion engine with a belt from a crankshaft, and compress the air flow to the engine cylinder with mechanical power provided by the engine. Most of conventional superchargers employ a positive displacement compressor rather than a centrifugal compressor because of the operating speed restricted by the engine rotation. The demerits of the positive displacement compressors are low-efficiency and low boost pressure.

In this study, therefore, an electric drive of the supercharger with the centrifugal compressor is investigated. The electric supercharger is assumed to be used with a 1.5-2.0-liters gasoline engine. Table 1 shows design specifications of the UHS PM motor discussed in this paper. Several problems of the motor should be resolved to achieve the UHS operation. At first, the electric supercharger is driven by a low voltage battery (12 V), which is used in most of conventional cars. Next, UHS drive generates much loss, for example, magnet eddy-current loss that is proportional to square of the operating frequency, and mechanical loss. Also, it is important to pay attention to mechanical vibration of the UHS drive.

Table 1. Design specifications of ultra-high speed PM motor.

Supply voltage (V)	12
Rated power (W)	1500
Rated torque (Nm)	0.0955
Rated speed (r/min)	150,000

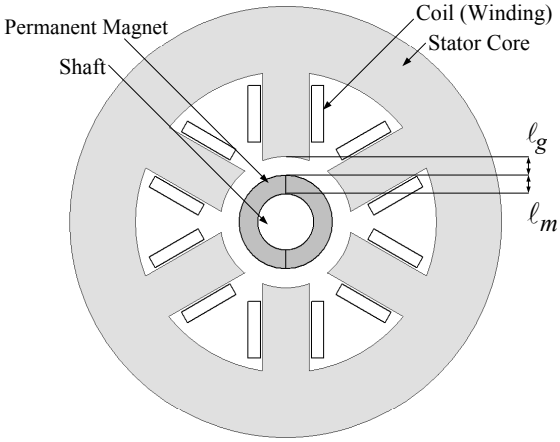

Figure 1. Configuration of ultra-high speed SPM motor.

2. Permeance coefficient and motor efficiency

Figure 1 illustrates the configuration of the UHS SPM synchronous motor. It mainly consists of a rotor shaft, a PM, windings, and a stator core. Several cases of the permeance

Table 2. Analysis conditions of UHS PM motors.

Type of shape	#1	#2	#3	#4	#5
Stator configuration	Concentrated winding				
Number of poles	2				
Number of stator slots	6				
Stator outer diameter (mm)	92				
Stator inner diameter (mm)	28				
Stator stack length (mm)	30				
Tooth width (mm)	10				
Airgap length (mm)	6	5	4	3	2
Magnet thickness (mm)	2	3	4	5	6
Permeance coefficient	0.33	0.60	1.00	1.67	3.00
Magnet, Br (T), iHc(kA/m)	Nd-Fe-B, 1.26, 954.9				
Rotor shaft diameter (mm)	12				
Thickness of steel sheet (mm)	0.1				
Operating current	Three-phase sinusoidal waveform				
Phase angle	In phase with e.m.f.				
FET ON resistance (mΩ/phase)	2				

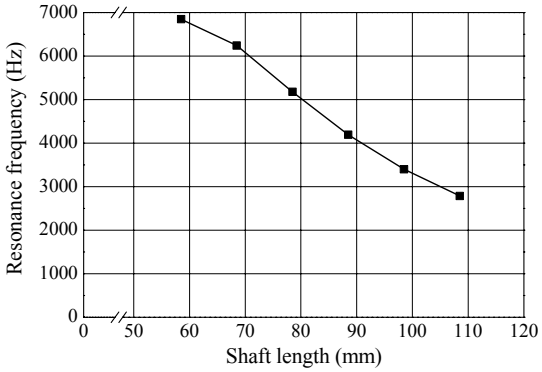

Figure 2. Relationship between shaft length and mechanical vibration.

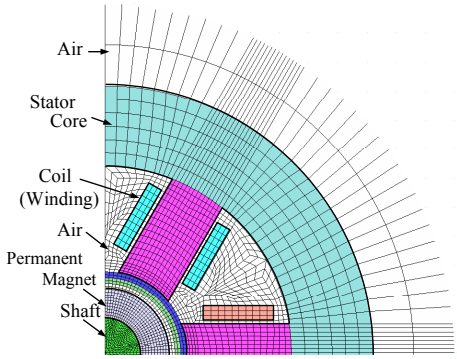

Figure 3. Mesh configuration of motor for FEM analysis.

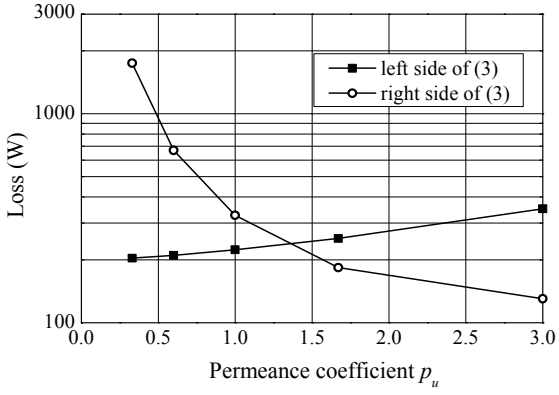

Figure 4. Comparison between both sides of Eq. (3) at rated operation.

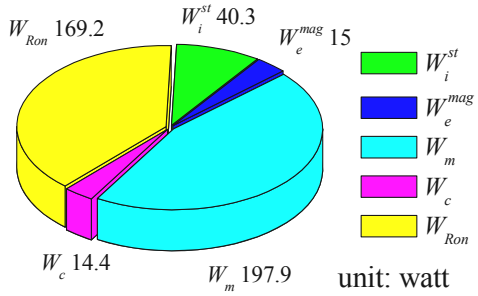

Figure 5. Loss analysis at maximum-efficiency operation.

coefficients shown in Table 2 are examined for design of the UHS motors. In the case of the SPM motor, the permeance coefficient is expressed by the following equation:

$$p_u = \frac{l_m}{a_m}\frac{a_g}{K_C l_g} \quad , \tag{1}$$

where l_m is a magnet thickness, a_m is an averaged cross sectional area of the magnet, a_g is an averaged cross sectional area of the air-gap between the rotor and the stator, l_g is an air-gap length, and K_C is a Carter's coefficient. For the SPM motor, a_g is nearly equal to $a_m K_C$, so (1) can be approximated as follows:

$$p_u = \frac{l_m}{l_g} \quad . \tag{2}$$

Therefore, the permeance coefficients are determined by only l_m and l_g. If other parts of motor shape are the same, the permeance coefficient is proportional to the motor electromotive force.

On the other hand, in order to improve the total efficiency of the motor drive system incorporating the inverter, the inverter loss must be taken into account. The maximum efficiency condition of the motor drive system can be described as (3).

$$W_i^{st} + W_e^{mag} + W_m = W_c + W_{Ron} \quad , \tag{3}$$

where W_i^{st} is an iron loss of the stator core, W_e^{mag} is an eddy-current loss of the rotor magnet, W_m is a mechanical loss which is bearing friction loss, W_c is a copper loss of the stator coil, and W_{Ron} is a conduction loss of the inverter. The left side terms of (3) don't depend on the drive current, while the right side terms are proportional to square of the drive current. Inverters have not only the conduction loss W_{Ron} but also a switching loss. The switching loss is proportional to the drive current, so it doesn't affect the maximum efficiency condition shown in (3).

3. Analysis results

3.1 Optimisation of permeance coefficient

Table 2 shows analytical conditions of the UHS motor to be investigated. Those motors are designed from the viewpoint of the specifications in Table 1, implementation in vehicles, and prevention of the mechanical vibration.

Permeance coefficient is changed from 0.33 (#1) to 3.00 (#5) according to configurations of l_m and l_g. The stator stack length shown in Table 2 is one of the most important parameter, and is fixed at 30 mm. Because the shaft vibration frequency should be higher than the motor operating frequency (2500 Hz). Figure 2 shows the relationship between the shaft length and the shaft vibration frequency. When the stator stack length is 30 mm, the shaft length is 78 mm, and the shaft vibration frequency is about 5200 Hz, which is more than twice of the operating frequency. Figure 3 illustrates a mesh configuration of the motor for 2D FEM analysis. It consists of 7692 elements and 7909 node points. Besides, it is analyzed at 3-degree intervals.

Figure 4 shows two kinds of losses when the designed motor is operated at the rated load. One is the left side of (3), which is summation of the iron loss W_i^{st} , the magnet eddy-current loss W_e^{mag}, and the mechanical loss W_m. The

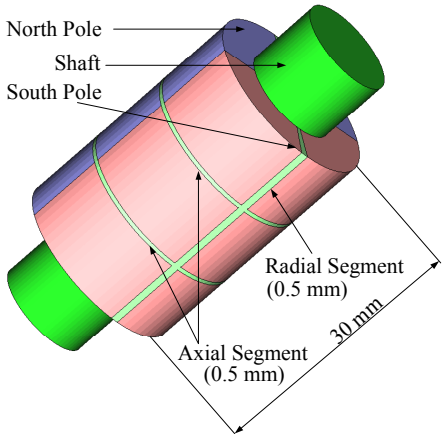

Figure 6. Configuration of PM segmentation.

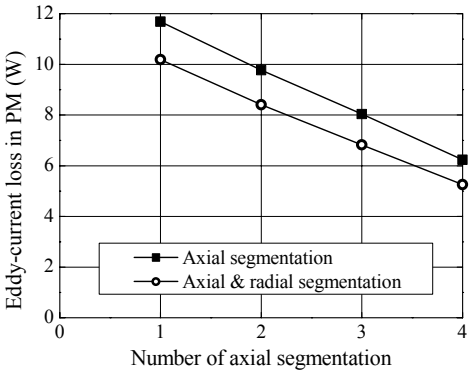

Figure 7. Relationship between magnet segmentation and eddy-current loss in PM.

other is the right side of (3), which is summation of the copper loss W_c and the inverter conduction loss W_{Ron}. Figure 4 shows a trade-off between the left side and the right side of (3) as the permeance coefficient is changed. In the case where the permeance coefficient is 1.4 (cross point of two curves shown in Figure 4), (3) is fulfilled and its efficiency becomes the maximum value.

The calculated system loss of #4 in Table 2 is indicated in Figure 5. For #4, the permeance coefficient value is the closest to 1.4. The system efficiency is 77.3 % which is a product of the motor efficiency (84.7 %) and the inverter efficiency (91.2 %). Figure 5 also shows that the mechanical loss and the inverter loss are dominant.

3.2 Loss reduction by means of magnet segmentation

The percentage of the magnet eddy-current loss is only 3.4 % as shown in Figure 5. However, the loss leads to magnet temperature rise and degradation of magnet performance, which is called "irreversible demagnetization." Therefore, the effect of magnet segmentation shown in Figure 6 is investigated. Electrical insulation material (0.5-mm width) is set to radial direction and axial direction between the magnets shown in Figure 6.

Figure 7 shows 3D FEM analysis results depending on the magnet segmentation. The magnet eddy-current loss is apparently reduced by 36.9 %, when the magnet is separated into three pieces in the axial direction. The

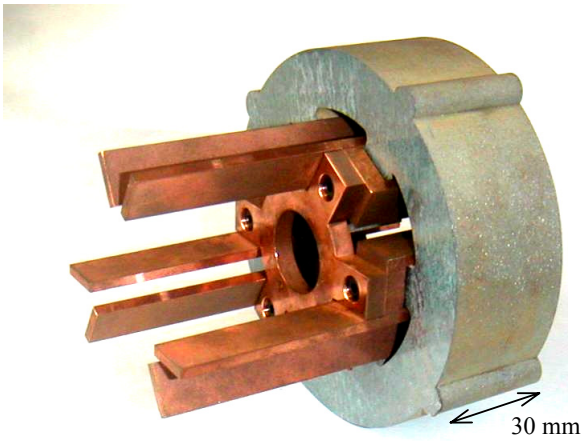

Figure 8. Prototype stator core and six 1-turn windings.

magnet eddy-current loss is reduced by 47.6 %, when the magnet is separated into two pieces in the radial direction in addition to the axial segmentation. The magnet segmentation of these six pieces reduces only 1 % with respect to the total system loss. However, the magnet segmentation is effective to reduce the temperature rise and to prevent the irreversible demagnetization of the magnet because the magnet loss can necessarily be decreased.

4. Conclusion

This paper describes a design of a 150,000 r/min-1.5 kW ultra-high speed permanent-magnet synchronous motor for a supercharger mounted on an automotive engine. The permeance coefficient is used for a design parameter, and the optimal shape of the motor is examined using FEM analysis. The trade-off between the left side terms and the right side terms of (3) has been calculated through FEM analysis. As a result, the system efficiency of the motor drive has been improved when the permeance coefficient is set so that (3) is satisfied. The efficiency of designed ultra-high speed motor has been achieved 77.3 %. In addition, it is found through 3D FEM analysis that the eddy-current loss of the rotor magnet is reduced by 47.6 % when the magnet is separated into six parts.

Feasibility of the analysis results described above is required, using a prototype of the real machine. The prototype shown in Figure 8 will be examined in detail in the future works.

References

[1] Noguchi, T., Takata, Y., Yamashita, Y., and Ibaraki, S., 2005. 160,000-r/min 2.7-kW Electric Drive of Supercharger for Automobiles. The Sixth International Conference on Power Electronics and Drive Systems, pp. 1380-1385.

[2] Noguchi, T., Takata, Y., Yamashita, Y., Komatsu, Y., and Ibaraki, S., 2005. 220,000-r/min 2-kW Permanent Magnet Motor Drive for Turbocharger. IEEJ Trans. on Industry Applications, Vol. 125, No. 9, pp. 854-861.

[3] Okawa, M., 1989. Design Manual of Magnetic Circuit and PM motor. Sogo Research Co., Ltd., Japan.